#### **CONFERENCE PRE-PRINT**

# SELF-ORGANIZED FRC FORMATION IN MIRROR FIELD ORTHOGONAL TO THE AXIS OF COUNTER-INJECTED PLASMOID

<sup>1,2</sup>T. Asai

<sup>1</sup> College of Science and Technology, Nihon University, Tokyo 101-8308, Japan

<sup>2</sup> LINEA Innovations, Inc., Tokyo 106-6115, Japan

Email: asai.tomohiko@nihon-u.ac.jp

<sup>1</sup>T. Takahashi, <sup>2</sup>Y. Miyamoto, <sup>1</sup>Y. Takeuchi, <sup>1</sup>R. Kikuchi, <sup>1</sup>D. Kobayashi, <sup>1,2</sup>T. Seki, <sup>3</sup>T. Takahashi, <sup>4</sup>M. Inomoto, <sup>5</sup>Y. Kishimoto, <sup>6</sup>N. Mizuguchi, <sup>2</sup>M. Mizuguchi, and <sup>2,7</sup>M. Sakamoto

- <sup>1</sup> College of Science and Technology, Nihon University, Tokyo 101-8308, Japan
- <sup>2</sup> LINEA Innovations, Inc., Tokyo 106-6115, Japan
- <sup>3</sup> Graduate School of Engineering, Gunma University, Gunma 376-0052, Japan
- <sup>4</sup> Graduate School of Frontier Sciences, The University of Tokyo, Chiba 277-8561, Japan
- <sup>5</sup> Graduate School of Energy Science, Kyoto University, Kyoto 611-0011, Japan
- <sup>6</sup> National Institute for Fusion Science, Gifu 509-5292, Japan
- <sup>7</sup> Plasma Research Center, University of Tsukuba, Ibaraki 305-8577, Japan

#### Abstract

We report the first demonstration of self-organized formation of an FRC-like high- $\beta$  plasmoid inside a mirror magnetic field via high-speed collisional merging of two plasmoids that are counter-injected along a common line orthogonal to the mirror-field axis. Unlike conventional axisymmetric FRC merging along the device axis, our approach injects two plasmoids perpendicular to the mirror-field axis, potentially leaving both axial ends available for reactor-relevant components (e.g. divertors or direct energy converters). In the FAT-CM device, deuterium plasmoids with a line-integrated density of (1–1.5)  $\times$   $10^{20}$  m $^{-2}$  were accelerated to  $\sim$ 150 km s $^{-1}$  each and merged at a relative speed of  $\sim$ 300 km s $^{-1}$ , creating a high-density region directly within the mirror field. Diagnostics (excluded-flux probes, internal magnetic probes, interferometry, and ion Doppler spectroscopy) show reversal of the poloidal field, transition from paramagnetic to diamagnetic rotation, and subsequent spin-up—all characteristic of self-organization observed in axial merging as well. The merged plasmoid exhibits a confinement time of  $\sim$  130  $\mu$ s, significantly exceeding the simple-mirror diffusion time (< 60  $\mu$ s at mirror ratio  $R\sim$ 2.9) , implying a closed-field structure that suppresses cross-field losses. These results suggest a feasible pathway toward mirror-FRC hybrid operation and may broaden options for FRC formation and high-speed fueling in linear systems, while leaving the axial ends potentially available for reactor-relevant components.

#### 1. INTRODUCTION

A field-reversed configuration (FRC) plasma combines axial symmetry, a simply-connected topology, and high- $\beta$  confinement, making it a compelling basis for compact fusion concepts [1,2]. Recent advances—axisymmetric collisional merging, scrape-off layer (SOL) control (edge biasing), and neutral-beam injection (NBI)—have enabled high-performance, beam-driven FRCs and renewed interest in advanced fuels (e.g. p- $^{11}$ B) [3,4]. In earlier FAT-CM studies, self-organization during merging process—including field-reversal reformation, ion-flow reorganization, and rapid conversion of kinetic energy into thermal and magnetic energy—has been clearly observed, reinforcing the view that collisional merging can robustly create relaxed, high- $\beta$  states [5].

Despite these advances, conventional axisymmetric merging intrinsically consumes both axial ends of the device for formation hardware, thereby constraining the integration of reactor-relevant components such as divertors and direct energy converters (DEC) and limiting operational flexibility [3,6]. Moreover, FRC equilibrium and stability are sensitive to the density and temperature of the surrounding open-field-line regions (SOL/halo). When the axial ends are occupied, active control of these peripheral regions is hindered, which complicates performance optimization and increases sensitivity to

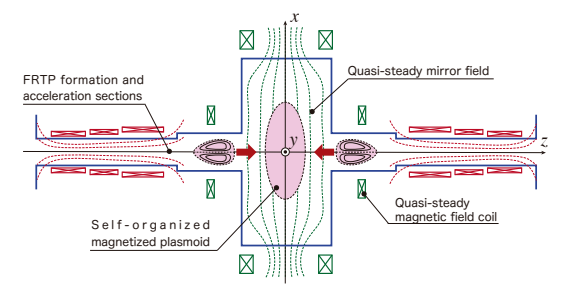


FIG.1. Conceptual diagram of the FAT-CM device and the orthogonal collisional-merging scheme in a mirror magnetic field.

wall and boundary conditions. These constraints motivate alternative formation routes that both preserve the axial ends and enable selective control of the near-field edge/SOL environment.

In this work, we explore a new formation topology: two FRC-like plasmoids are generated in FRTP-type conical theta-pinch sections, accelerated, and injected orthogonally into a mirror magnetic field in the central confinement region. By design, the transverse injection cancels axial momenta at impact, concentrates energy deposition directly inside the mirror field, and allows both device ends to remain free for reactor components and edge-control systems. As we show below, the orthogonal collisional merging produces a reversed-field structure, a paramagnetic to diamagnetic rotation transition, and spin-up analogous to axial merging, while the observed lifetime (~130 μs) exceeds the simple-mirror diffusion time (< 60  $\mu$ s at  $R \sim 2.9$ ), indicating a closed-field, high-β configuration. This mirror-FRC hybrid approach therefore opens a complementary path to high-performance targets for NBI in linear systems and broadens reactor design space by decoupling formation from the axial ends.

#### 2. EXPERIMENTAL APPARATUS

Experiments were conducted on the FAT-CM device (Figures 2(a)-(b)). The system comprises two formation-and-acceleration sections based on an FRTP-type conical  $\theta$ -pinch and a central confinement

Helmholtz coil

Mirror coil

Acceleration coil

Auxiliary coil

Conical theta-pinch coil

Internal

Magnetic Probe (IMP)

(x = 0, internal of y = 0.04 m)

Excluded magnetic flux probe

(x = 0.15 m)

Excluded magnetic flux probe

(x = 0.2 m, viewing chord of 0.1 m)

Excluded magnetic flux probe

(x = 0.2 m, viewing chord of 0.1 m)

Excluded magnetic flux probe

(x = 0.2 m, viewing chord of 0.1 m)

(x = 0.15 m)

Acceleration coil

Auxiliary coil

Lon Doppler Spectroscopy (IDS)

(x = 0.2 m, viewing chord of 0.1 m)

Excluded magnetic flux probe

(x = 0.15 m)

Acceleration coil

Auxiliary coil

Lon Doppler Spectroscopy (IDS)

(x = 0.2 m, viewing chord of 0.1 m)

Excluded magnetic flux probe

(x = 0.15 m)

Acceleration coil

Auxiliary coil

Lon Doppler Spectroscopy (IDS)

(x = 0.2 m, viewing chord of 0.1 m)

FIG. 2. FAT-CM hardware and diagnostics: (a) experimental setup for orthogonal (vertical) plasmoid injection into a mirror magnetic field; (b) diagnostic layout for the collisional-merging experiments.

section that provides a mirror magnetic field transverse to the plasmoid-injection axes. The aim is to investigate whether orthogonal, high-speed collisional merging can broaden the options for forming an FRC-like high- $\beta$  plasmoid directly inside a mirror field, in a way that may keep the axial ends available for engineering functions (e.g. divertors/DECs) and rapid fueling.

Each formation section uses a conical θ-pinch approximately 1 m in length with an opening angle of 1.72 degrees realized by arranging coils of inner diameters of 18, 17, 16 and 15 cm. A pair of auxiliary coils assists reconnection control at the coil ends [7]. The formation vessel is fused quartz (ID 0.256 m, length 1.5 m). An acceleration coil is wound directly on the vessel (ID 0.256 m, length 0.3 m). These sections generate FRC-like plasmoids that are then accelerated by magnetic-pressure gradients toward the central confinement region [8].

The confinement region employs Helmholtz-like coils (z = 0.62 m,  $x = \pm 0.235$  m) and mirror coils (z = 0.275 m,  $x = \pm 0.874$  m) that are independently powered, permitting separate control of the mirror ratio (R) and the transverse confinement-field strength. The confinement vessel is SUS304 (ID 0.775 m, length 2.0 m, thickness 4 mm). Field calculations (Fig. 4) indicate  $B_x \sim 0.08-0.04$  T across the mid-plane, a mirror spacing ~2.2 m, and  $R \sim 2.9-5.8$ ; typical operation in this study used  $R \sim 2.9$ . From the maps in Fig. 4(a) and (b), injected plasmoids encounter a magnetic-pressure barrier from the transverse field in -0.8 m  $\lesssim z \lesssim 0.8$  m before entering the confinement region.

Excluded-flux probe arrays were installed at x = 0,  $\pm 0.3$ ,  $\pm 0.6$  m in the confinement vessel to estimate the evolving excluded-flux radius ( $r_{\rm ex}$ ). A 3.39  $\mu$ m He–Ne heterodyne interferometer was located near the exit of each formation section to monitor injected-plasmoid density and at z = 0, x = 0.05 m to capture density after merging. Internal B-probe arrays were positioned at z = 0, x = 0 with sampling along y, and at z = 0, x = 0.25, -0.05, -0.35 m to track the reversed-field structure near the vessel axis. Ion Doppler spectroscopy (IDS) measured ion temperature/flow at x = 0.1 m, z = 0.2 m. A high-speed camera at x = -1.0 m, z = 0 recorded end-on dynamics in the transverse field. This diagnostic set enables cross-validation of topology (excluded flux), magnetic structure

(magnetic probes), and flow/temperature (IDS), while imaging provides qualitative context for rotation and deformation.

#### 3. EXPERIMENTAL RESULTS

Figures 4 (a) and (b) show  $r_{\rm ex}$  contours or single-sided operation, demonstrating acceleration of FRC-like plasmoids from both formation sections. With orthogonal injection into the mirror field, the two plasmoids collide and merge in the confinement region [Fig. 4(c)]. In typical shots, deuterium plasmoid with a line-integrated density of  $1{\sim}1.5\times10^{20}$  m $^{-2}$  were accelerated to approximately 150 km s $^{-1}$ ; merging occurred at a relative velocity of 300 km s $^{-1}$ . After collision, the merged structure expands along x, reflects at the mirror throats, contracts, and then re-forms. These motions appear robust over the operating window explored here.

High-speed imaging (Fig. 5) reveals that immediately after collision the plasma rotates in the paramagnetic direction, then, within several frames ( $\Delta t \sim 1.5 \,\mu\text{s}/\text{frame}$ ), transitions to diamagnetic rotation with evident spin-up. Reversing the sign of  $B_x$  produces the same sequence (paramagnetic to diamagnetic), indicating that the behavior is insensitive to field polarity. Consistently, internal magnetic probes (Fig.

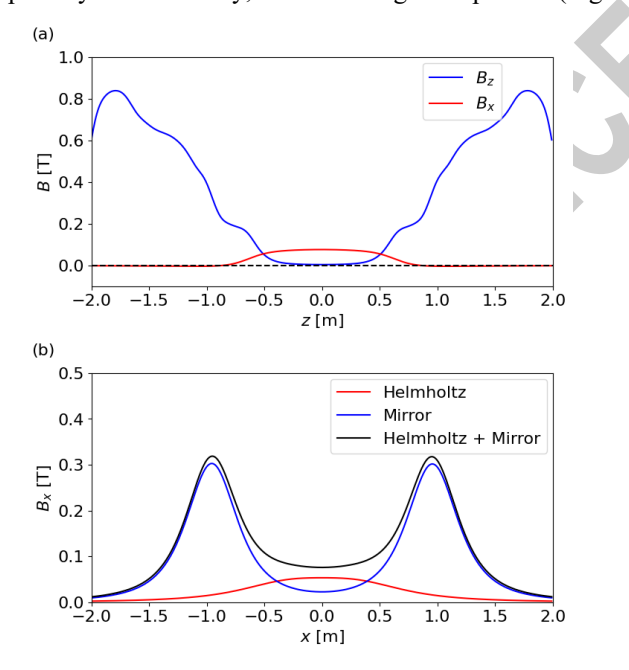


FIG. 3. Magnetic-field distributions in the FAT-CM device: (a)  $B_z$  (blue) along the formation/acceleration axis with overlaid transverse confinement field  $B_x$  (red), illustrating the magnetic-pressure barrier that injected plasmoids must overcome; (b)  $B_x$  along the confinement-vessel axis, showing contributions from the mirror coil (red), Helmholtz coil (blue), and the total field (black).

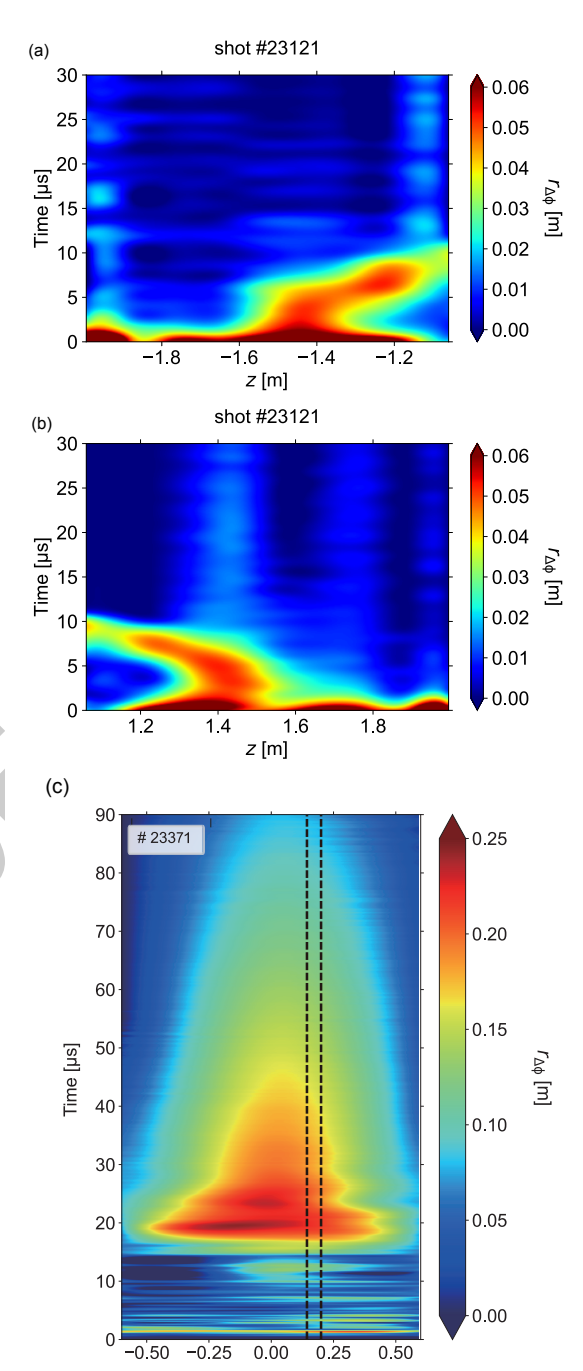


FIG. 4. Time evolution of the excluded-flux radius  $(r_{ex})$  measured by the probe array: (a) injection from the R-side formation region only; (b) injection from the V-side formation region only; and (c) orthogonal injection with collision/merging in the confinement region. Black dashed lines at x = 0.15 m and x = 0.20 m indicate the internal B-probe insertion location and the viewing chord of IDS, respectively.

6(a)) show a reversed-field structure emerging soon after collision, temporarily disappearing, and then reappearing, while  $r_{\rm ex}$  (Fig. 6(b)) peaks at impact, contracts, grows again, and finally decays. The IDS (Fig. 6(c)) shows a ~20  $\mu$ s delay between collision and the paramagnetic to diamagnetic transition, followed by spin-up. These observations—the reversed-field signature, rotation reversal, and spin-up—are consistent with self-organization reported in axial merging and FRTP-formed FRCs [5,9,10].

From  $r_{\rm ex}$  decay and probe comparisons, the merged plasmoid persists for ~130 µs. For reference, simple-mirror diffusion times estimated for the present conditions (deuterium,  $R \sim 2.9$ ,  $n_{\rm e} \sim 0.5 \times 10^{20}$  m<sup>-3</sup>,  $T_{\rm i} \sim 100$ –200 eV) are < 60 µs (Table 1). The observed lifetime therefore exceeds the simple-mirror expectation by more than a factor of two, suggesting a closed-field structure with reduced parallel loss. We note that probe insertion can perturb local fields and thus interpret single-point  $B_x$  wavef orms with caution

The IDS measurement indicates  $T_i \sim 100-200$  eV, and interferometry at the mid-plane gives  $n_e \sim 0.5 \times 10^{20}$  m<sup>-3</sup> during the quasi-stationary phase. The merged plasmoid translates while maintaining diamagnetic rotation, consistent with a high- $\beta$  state. While full equilibrium reconstruction is beyond the present scope, the combined magnetic and flow diagnostics support the presence of a reversed-field, high- $\beta$  configuration during the growth and plateau phases preceding decay.

#### 4. DISCUSSION AND SUMMARY

The observed plasma lifetime was compared with the diffusion due to the mirror-loss. Using standard loss-cone-limited mirror-diffusion formulae that scale with the ion-ion collision time [11], the diffusion time  $\tau_D$  is expressed as

For isotropic diffusion:

$$\tau_{D\_iso} = 1.57 \frac{\ln\left(\cot\frac{\theta_0}{2}\right) - \cos\theta_0}{\cos\theta_0} \tau_i \tag{1}$$

For radial diffusion:

$$\tau_{D\_rad} = 1.57 \frac{\ln\left(\frac{1}{\sin\theta_0}\right)}{\cos\theta_0} \tau_i \sim 0.78 (\ln R) \tau_i \quad (2)$$

Here,  $\theta_0$  is the loss-cone angle at the mid-plane, related to the mirror ratio R via  $\sin^2 \theta_0 = 1/R$ ;  $\tau_i$  is the ion–ion collision time evaluated at the local plasma parameters; and ln denotes the natural logarithm. Equation (1) corresponds to the isotropic case and Eq.

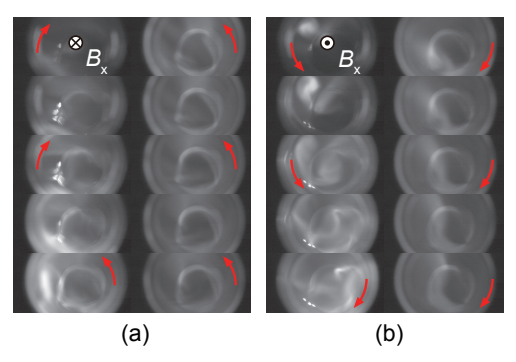


FIG. 5. High-speed, end-on images of orthogonal (vertical) collisional merging (frame spacing 1.5  $\mu$ s; panels progress left-to-right and top-to-bottom). Left: confinement field  $B_x$  along  $\neg x$ . Right:  $B_x$  along +x.

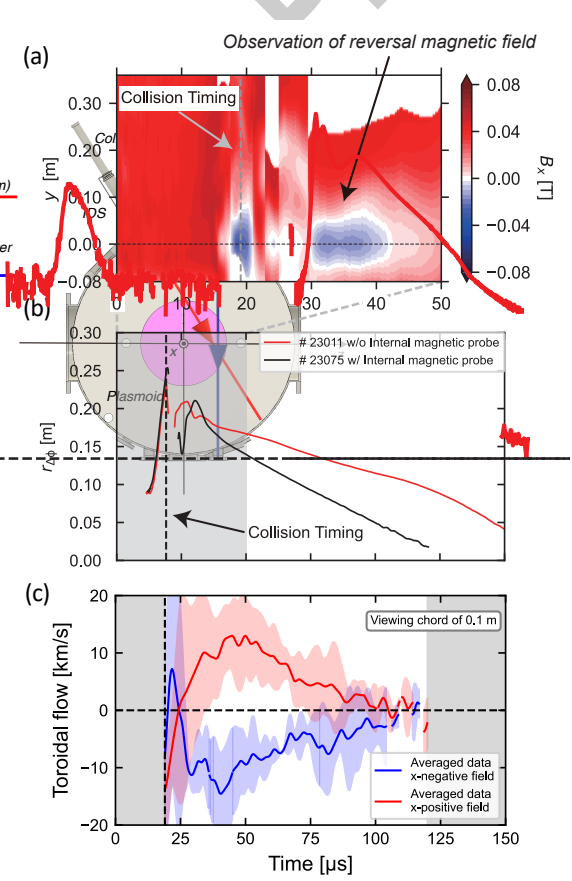


FIG. 6. Characteristics of orthogonally injected plasmoids: (a) contour of the poloidal field  $B_y$  versus time from the internal B-probe array; (b) time evolution of the excluded-flux radius  $r_{ex}$  near x = 0, z = 0; (c) IDS-inferred ion-flow evolution. Here, positive flow is taken in the ion diamagnetic direction due to the  $B_x$ -positive field.Red and blue traces correspond to  $B_x$  along +x and -x, respectively.

TABLE 1	COMPINIEN		OF SIMPLE MIRRO	n
IABIEI		/	OF SIMPLE MIRRO	к

Diffusion Time	τ <sub>D</sub> [μs]				
Mirror Ratio R	5.1		2.9		
Plasma Parameter	isotropic	radial	isotropic	radial	
$n = 5 \times 10^{19} \mathrm{m}^{-3},$ $T = 200 \mathrm{eV}$	62.6	91.6	39.4	66.2	
$n = 1 \times 10^{20} \text{ m}^{-3},$ T = 100  eV	11.4	16.4	7.10	12.0	

(2) to the radial case used in Table 1. With the present operating point ( $R \sim 2.9$ ), Eqs. (1)–(2) yield  $\tau_D \lesssim 60$  µs, consistent with Table 1.

In contrast, the merged plasmoid persists for  $\sim$  130  $\,\mu s,\,$  i.e., more than twice the simple-mirror estimate. Together with the reversed-field signatures and diamagnetic spin-up, this supports the interpretation that the merged state attains a closed-field, relaxed configuration with suppressed parallel losses.

Figure 7 shows the time evolution of  $B_{\rm ex}$  at x=0.15 m on the x-axis (z=0). A representative change from  $B_{\rm ex}=0.075$  T to  $B_{\rm in}=0.065$  T near the mid-plane implies a toroidal current density per unit length of  $J_{\theta} \sim (B_{\rm ex}-B_{\rm in})/\mu_0 \sim 110$  kA m<sup>-1</sup>. With  $n_{\rm e} \sim 5 \times 10^{19}$ 

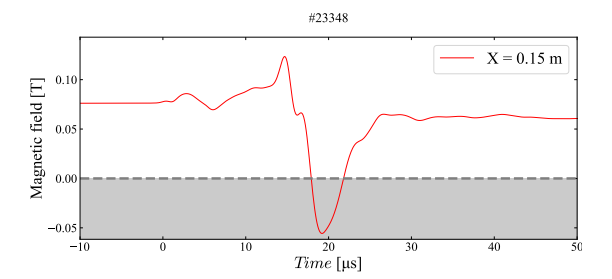


FIG. 7. Time evolution of magnetic flux density observed by an internal magnetic probe installed at x = 0.15 m, z = 0, inserted from the x-axis direction

m<sup>-3</sup>,  $T_{\rm i} \sim 100-200$  eV, and an empirical  $T_{\rm total} \sim 1.2~T_{\rm i}$ , pressure-gradient estimates  $|\nabla P|$  give diamagnetic currents of order  $10^2-10^{2.5}$  kA m<sup>-2</sup> [12], compatible with the reversed-field indicated by internal probes. Because probe insertion can locally perturb the field (Figs. 6 and 7), these current values are treated as order-of-magnitude estimates.

These results indicate that two plasmoids, counter-injected along the same line (coaxial), where that injection line is orthogonal to the mirror-field axis, can merge inside the mirror field to form a high- $\beta$ , FRC-like plasmoid whose lifetime can substantially exceed simple-mirror diffusion estimates. This geometry decouples the merging (injection) axis from the confinement (mirror) axis and thus may broaden the operational space for FRC formation and high-speed fueling in linear/mirror systems—potentially keeping the ends of the mirror axis available for reactor-relevant components (e.g., divertors, DECs) and edge/SOL control hardware. Future work will clarify performance limits and scalability through systematic scans of R, edge/SOL biasing, and coupling to NBI.

## **ACKNOWLEDGEMENTS**

The authors are grateful to the members of the Plasma Physics Laboratory at Nihon University for expert assistance with experiments and for support with diagnostics. This work was partially supported by JSPS KAKENHI Grant No. JP20H00143 and by Nihon University through the College of Science and Technology's Grant for Project Research and Grant for the Promotion of Leading Research.

### REFERENCES

- [1] M. Tuszewski, Nucl. Fusion 28, 2033 (1988).
- [2] L. C. Steinhauer, Phys. Plasmas 18, 07501 (2011).
- [3] H. Gota et al., Nucl. Fusion **64**, 112014 (2024).
- [4] R. Magee et al., Nat. Commun. 14, 955 (2023).
- [5] T. Asai et al., Nucl. Fusion 61, 096032 (2021).

#### IAEA-CN-316/INDICO ID

[Right hand page running head is the paper number in Times New Roman 8 point bold capitals, centred]

- [6] H. Gota et al., Nucl. Fusion **59**, 112009 (2019).
- [7] T. Asai et al., Nucl. Fusion 64, 096013 (2024).
- [8] D. Kobayashi et al., Plasma Phys. Control. Fusion 66, 065017 (2024).
- [9] T. Asai et al., Phys. Plasmas 31, 010703 (2024).
- [10] R. Kikuchi et.al., Phys. Plasmas 32, 010501 (2025).
- [11] D.V. Sivukhin, Rev. Plasma Phys. 4, 93 (1966).
- [12] H. Y. Guo et al., Phys. Plasmas 18, 056110 (2011).

